Journal of Physics: Conference Series **2391** (2022) 012006 doi:10.1088/1742-6596/2391/1/012006

Operation of an Energy Recovery Linac with an Internal Target

S V Benson[1] and D R Douglas[2]

[1] Thomas Jefferson National Accelerator Facility, Newport News, VA 23606
[2] David R. Douglas Consulting, Yorktown VA 23690

E-mail: felman@jlab.org

Abstract. Because an Energy Recovery Linac (ERL) decelerates and dumps the beam after at most a few passes, beam degradation in the interaction region that is orders of magnitude larger than in a storage ring is tolerable in such a device. As a consequence, some new types of Nuclear Physics experiments can be carried out. In 2016, an experiment (the DarkLight experiment) was installed in the Jefferson Lab FEL Driver ERL to test out this idea. The ERL had previously been used for FEL applications where high peak current and a large growth in energy spread was present. For the internal target, the machine setup required very small energy spread, and had to deal with large transverse emittance growth in the target. Additionally, the addition of a strong solenoid in the transport complicated the details of energy recovery. This presentation will describe how these new machine physics challenges were addressed.

1. Introduction

Internal target experiments to date have generally been carried out in storage rings [1]. We describe here an attempt to use an Energy Recovery Linac (ERL) to provide an opportunity to increase the density of the internal target by several orders of magnitude. An ERL can tolerate beam losses of as much as 0.1% after the target if they are in a well-shielded dump. This means that the target may be much thicker than in a storage ring, where losses must be very small ($\ll 1$ ppm per pass).

Another advantage of an ERL for internal target experiments is the ability to operate at very low energies. Dark Matter experiments often operate at low center-of-mass energy to restrict the phase space of the interaction [2]. Storage rings suffer from intra-beam-scattering (IBS) at low energy, limiting available beam brightness [3]. An ERL can provide much smaller emittance and energy spread since the beam only traverses the interaction region beamline and target once.

The DarkLight experiment embedded a 0.77 m long dense gaseous hydrogen target and detector package in a 1.1 m solenoid operating with 5 kG field [4]. A series of baffles, with small (3 mm diameter) apertures and differential pumps isolated the target from the ERL transport system [5]. The spent beam was transported from the target/detector to the downstream recovery line through a "Møller dump" that absorbed large-amplitude Møller-scattered electrons and collimated them using rings of carbon and tungsten. The ERL transport system then had to be optimized to provide sufficient control of the beam to the target, adequate downstream acceptance (both transverse and longitudinal) to handle the beam after interaction with the target, and control of solenoid-induced coupling so as to manage both beamline optics and the beam breakup instability. This combination of constraints was most readily satisfied by

locating the experiment in the infrared FEL region of the ERL [6], with the experimental package replacing the infrared wiggler and appropriate modifications of the upstream and downstream transport providing the necessary phase space management (see figure 1-3).

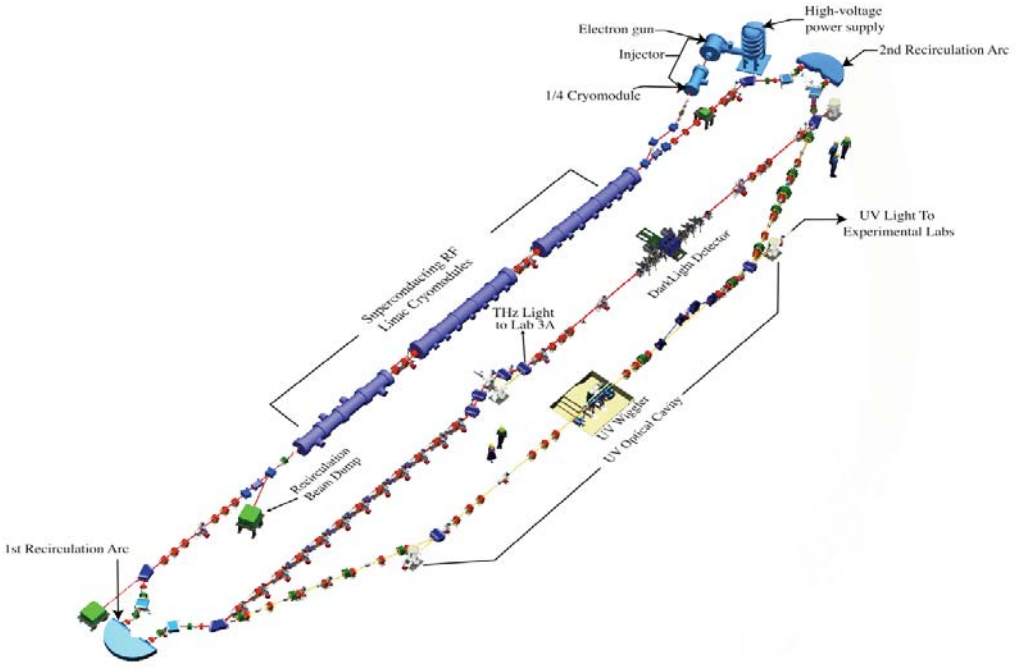

Figure 1. Jefferson Lab Energy Recovery Linac with DarkLight experiment embedded in the former Infrared FEL location.

Figure 2. Detail of the interaction region of the DarkLight experiment showing the 12 regular and 10 skew quadrupoles used to match into and out of the solenoid (blue cube) and rotate the transverse phase space to reduce the Beam Breakup instability.

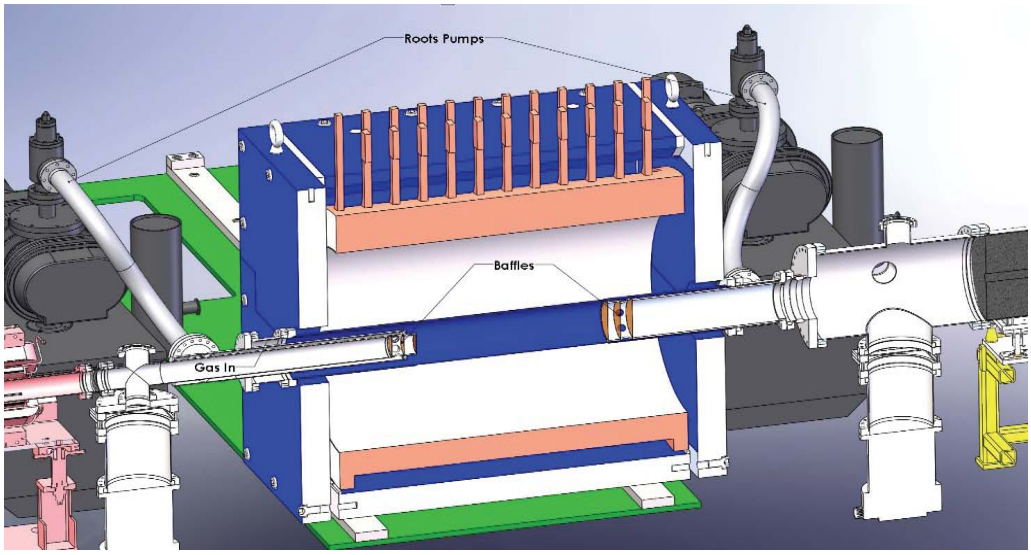

Figure 3. Detail of the interaction region of the DarkLight experiment. The Møller dump is on the far right and has a 1 cm graphite and tungsten aperture to capture scattered electrons.

2. Requirements

Ideally, the ERL transport system together with the target package should meet a simple set of requirements:

(i) The longitudinal match will provide a long bunch with small momentum spread to the target. This minimizes wake and resistive wall heating and provides narrow energy bandwidth for the user. The exhaust bunch will have a slightly degraded energy spread due to interaction with the target.

(ii) The target will be "thin" – in the sense that little betatron motion occurs over its length.

(iii) To avoid scattering-induced coupling, the beam will be uncoupled at the target. Thus, the linac to solenoid-center transport will be uncoupled and the solenoid-center to linac transport will be uncoupled.

(iv) To suppress Beam BreakUp (BBU), the linac-to-linac transport will exchange transverse phase spaces. This exchange is accumulated in the match to the target, the solenoid, and the match from the target.

(v) The beam will be matched into the solenoid with an upright phase space ($\alpha_{Twiss} = 0$) at the characteristic Twiss envelope value for a solenoid (twice the Larmor radius).

(vi) With the beam uncoupled at the "short" target, scattering will notionally not introduce coupling, so the target will transform the transverse phase spaces in a manner discussed elsewhere [7] and the beam from the target forward is characterized by an emittance increased - and a Twiss beta decreased - by the ratio of the incoming to outgoing angular divergences. Downstream betatron acceptance will be set to accommodate this exhaust phase space.

We note that an electron scattered within the solenoid will undergo motion characteristic of a magnetized beam. However, instead of a linear combination of the desirable "magnetized" eigenmodes, which follow solenoid field lines, it instead enters into a linear combination of the orthogonal "Larmor" eigenmodes (which are "magnetized" eigenmodes for a solenoid of opposite polarity) and precesses around field lines.

Table 1. Beam and Machine Parameters for DarkLight experiment.

Parameter (Unit)	Value
e- Beam Momentum (MeV/c)	100
Normalized Emittance (mm-mrad)	
upstream	8
downstream	~ 40
RMS Bunch Length (psec)	2.5
RMS Full-Energy $\frac{\delta p}{p}$(%)	
upstream	0.03
downstream	0.1 [4]
Bunch charge (pC)	60
Rep rate (MHz)	75
Current (mA)	4.5
Solenoid Field (kG)	5
Solenoid Length (m)	1.1
Solenoid Matched	
$\beta(m)$	1.3343
$\alpha(rad)$	0
Solenoid Radial Aperture (m)	0.1
Target Length (m)	0.77

In Table 1 we summarize the specifications for the accelerator and target for the DarkLight experiment for the initial runs. The average current and repetition rate was chosen only because it was straightforward to achieve. Future experiments would benefit from a higher repetition rate of 150 MHz and higher average current of at least 9 mA.

3. Beam Matching

The beam/target interaction has specific consequences for the beam [8]:

(i) Single scattering dominates;
(ii) The target is "thick" – it acts on the beam over its full length of 0.77 m.
(iii) Scattering events result in losses of order 200-300 ppm in the downstream Møller dump (which has 1 cm diameter aperture and is 0.5 m full length).
(iv) Scattering events increase the beam energy spread from the initial 0.03% rms to 0.1% rms.

Taking these issues into account, the following design approaches were taken:

The solenoid and target were, in simulations, subdivided into multiple slices of 0.055 m length. Twenty slices were used to describe the solenoid. Single scattering was modeled at fifteen points between 16 of these slices by introducing a pair of transformations eliminating the fringe field of the up- and downstream slice solenoid maps [7], and embedding between the "antifringes" a transformation inflating the beam angular divergences and momentums spread by user-defined factors. Given the (assumed) axial symmetry of the optics, this scattering transformation was therefore of the following form:

$$\begin{pmatrix} 1 & 0 & 0 & 0 & 0 & 0 \\ 0 & F_{\text{transverse}} & 0 & 0 & 0 & 0 \\ 0 & 0 & 1 & 0 & 0 & 0 \\ 0 & 0 & 0 & F_{\text{transverse}} & 0 & 0 \\ 0 & 0 & 0 & 0 & 1 & 0 \\ 0 & 0 & 0 & 0 & 0 & F_{\text{longitudinal}} \end{pmatrix}$$

We note that this transformation is not symplectic, which is however consistent with the notion of scattering being a nonconservative process when viewed solely from the perspective of the beam. We also note that the anti-fringe transforms [7] are not symplectic when used with variables $x, x', y,$ and y'. This had consequences for the particular coupling management scheme that was used.

In practice, ray-tracing was used to establish working values for $F_{\text{tranverse}}$ and $F_{\text{longitudinal}}$. An initial beam distribution was defined and traced through the solenoid to the Møller dump, with the F factors changed at the first slice and the results recorded. This was repeated at each of the rest of the slices. The inflation factors were then increased until a) the integrated loss on the Møller dump from scattering at all slices was of order 200 to 300 ppm, and b) the output momentum spread from each (and all) slice(s) was 0.1% rms. The resulting distributions were then notionally consistent with those produced by the analysis of Ref. [8], and give rms beam divergences and energy spread at the solenoid exit of the order of earlier analytic estimates.

This analysis was for an ideal system. We had, however, to take into account some realities. First, the target was not short – it was long enough for electrons to respond in position to deflections from scattering. Secondly, the dynamics within a solenoid must be observant of the effects – or rather, the absence – of the solenoid fringe fields when the beam is scattered inside the solenoid [9] This had numerous consequences for the modeling of the system using conventional beam optics codes such as DIMAD. In particular, the solenoid maps in such programs inherently include fringe effects, so when subdividing the solenoid, provision for eliminating fringes in the interior must be made as described above. Given that in an (x,x',y,y') representation of the transverse phase space these descriptions are nonsymplectic, it was thus not possible to manage coupling compensation in the manner demanded by the above requirements.

As noted above, scattering in the solenoid interior put electron orbits into a linear combination of magnetized and Larmor modes [9]. The beam was therefore inherently coupled. Given that the transform from the interior of the solenoid back to the linac was nonsymplectic (by virtue of the anti-fringe fields in the solenoid), it was not possible to compensate this using solely a downstream quadrupole telescope (which can only produce symplectic transformations).

It was thus not possible to "orthogonalize" the optics solution; system requirements therefore had to introduce opportunity to optimally manage coupling (so as to control BBU) while still providing control over beam envelopes through the constrained apertures of the target and during energy recovery. The following set of requirements was found to allow this.

3.1. Accommodations for real-life effects

(i) The target was "thick": motion of electrons scattered in the front end of the target evolved significantly under the influence of the solenoid field. An analytic description is given in [8].

(ii) The beam – which was uncoupled at the front end of the interaction region – may be coupled at any point thereafter and *will* be coupled throughout the length of the target and solenoid. scattering may enhance the coupling. The recovery optics solution must be optimized to transport the degraded coupled beam to the dump.

(iii) Matching the beam to the solenoid entrance will – even for coupled beam – prevent beam envelope mismatch and limit overall beam size in the solenoid, providing optimal

transmission at the target aperture restrictions.

(iv) As the beam was coupled and the target was thick, scattering enhanced coupling and degraded emittance. However, the degradation – described in [8] – resulted in an exhaust beam with well-defined phase space characteristics, with moments (sigma matrix elements, including size and divergence) as well as specific patterns of coupling and distortion that inform optimization of the recovery betatron match. Downstream betatron acceptance was therefore tuned to accommodate this exhaust phase space.

(v) The Møller dump served to provide some degree of collimation of the exhaust electron beam. It was downstream of the detector solenoid, immediately upstream of the first quadrupole downstream of the solenoid, of length 0.5 m and 5 mm radial bore (1 cm diameter). Most of the beam clears the dump (see figure 4).

4. Accelerator Setup

Several accomplishments were required to carry out the DarkLight experiment:

(i) Clean beam had to be transported through six 3 mm holes in the Kapton foils. To ensure that we could accomplish this, we ran an aperture test to verify that we could run 500 kW of beam through a very small hole for hours at a time [10, 11].

(ii) We had to run with very small energy spread with full energy recovery. This involved accelerating off crest in first and third cryomodules and off-crest in the opposite direction in the middle cryomodule producing a smaller overall energy spread that could be quickly phased. The recovered beam was 180° out of phase with the accelerated beam. This longitudinal phase space match was tested out in the aperture test and worked well.

(iii) Scattering upstream of the target had to be minimized. This was done by careful matching of the beam and running the accelerator cavities at $\sim$ 6MV/m gradient so there would be no field emission.

(iv) We had to transport a low energy beam through a large 5 kG solenoid. This is straightforward if the solenoid is ideal. In our case there was an uncompensated conductor in the solenoid that produced a transverse field in the solenoid.

(v) As noted above, the phase space had to be rotated by 90 degrees to increase the BBU threshold. This is partly accomplished by the solenoid field but it is completed by 5 skew quadrupoles that rotate the beam by about 22 degrees before and after the solenoid. Several beam position monitors and viewers had to be added to the transport line to set up these skew quadrupoles;

The match to the solenoid (upstream telescope configuration) was developed as follows. The skew quadrupoles were set to provide a phase space rotation of 22° from the linac to the solenoid entrance. The match optimization was performed by putting a decoupling +45° roll at the center of the solenoid, and adjusting the quadrupoles to zero out the off-diagonal elements of the linac-to-solenoid-center transfer matrix ($M_{13} = M_{14} = M_{23} = M_{24} = M_{31} = M_{32} = M_{41} = M_{42} = 0$) while matching the beam envelopes to the acceptance of the solenoid. The latter constraint was most simply applied by injecting a matched decoupled beam of unit (1 m-rad) emittance into the start of the recirculator, and fitting the sigma matrix elements to the solenoid acceptance envelopes: $\Sigma_{11} = \beta, \Sigma_{12} = 0, \Sigma_{21} = 1/\beta, \Sigma_{33} = \beta, \Sigma_{34} = 0$, and $\Sigma_{44} = 1/\beta$. There were eight independent constraints on the eleven free parameters.

The match from the solenoid was rendered somewhat more complex by virtue of the need to manage beam that had been scattered by the target. The design/optimization process was therefore iterative The impact of scattering was initially treated as an impulsive increase the in the angular divergence of an upright matched beam at the very center of the solenoid. The downstream lattice was then matched to accept a beam with emittance scaled up by a

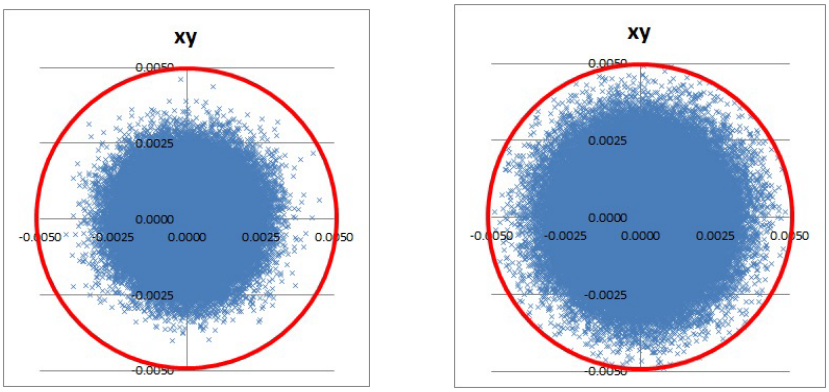

Figure 4. Beam profiles at the graphite entrance of the Møller dump (left) and at the Tungsten exit (right). The red circle represents the 1 cm diameter hole in the dump.

degradation factor, and beam envelope reduced by the same factor. In this case, the estimated emittance blowup was approximately a factor of four, so an upright beam ($\alpha = 0$) with envelope value of $\sim (1/4)\beta_{\text{solenoid}}$ was transported from the center through to the re-injection point of the linac, and two stages of matching were performed. The first stage set the 11 quads immediately downstream of the solenoid; these were optimized to complete the phase space exchange and to generate an optimized lattice envelope match at the center of the return transport arc. As the phase space exchange is complete by the end of the target insertion region, the remaining transport is decoupled and described by the usual lattice parameters. In practice, these constraints were – as with the match to the solenoid – entered via the sigma matrix, in as much as the initial beam specification and upstream lattice are fully coupled. Again, the eleven quads are under-constrained by the eight independent target parameters, so some latitude was available in the optimization process; internal mismatch and aberrations were thereby afforded some control. The match for this setup is shown in figure 5. The beam was – in simulation – very well contained throughout the beampipe to the dump.

We then had to take into account the thickness of the target. The degradation factor $F_{\text{transverse}}$ was set by comparison to losses as evaluated in [8]; that is, it was adjusted to give 200-300 ppm loss in the Møller dump. $F_{\text{longitudinal}}$ is set to give 0.1% rms dp/p by the end of the solenoid.

Once the exhaust beam was thus defined, full optimization of the recovery match proceeded. The initial solution was used to propagate beam matrices and as the basis for raytracing. Beam matrices for scattering from each "slice" of the target were propagated and spot sizes evaluated. Particle losses and distributions at key locations – solenoid exit, linac reinjection point, and at the end of the linac – were generated and cross-checked with the beam matrix propagation. The reinjection match was adjusted to provide optimum transmission (that is, to minimize the envelope of the collection of all propagated spot sizes). The results of the final match are shown in figure 6. Though increased from the thin target, the overall beam size is still well confined.

Longitudinal phase space behavior was monitored during the matching process to ensure that the appropriate induced momentum spread was adequately managed during recovery. The impact of chromatic aberrations was evaluated to confirm that the matching process did not lead to excessive variation in relevant beam parameters.

5. Accelerator Performance

An attempt was made to energy recover beam with no hydrogen gas or foils. A reasonable match was achieved but CW beam was not run before adding the target foils due to lack of time.

The foils and hydrogen system were installed and we verified that up to 2 Torr of hydrogen

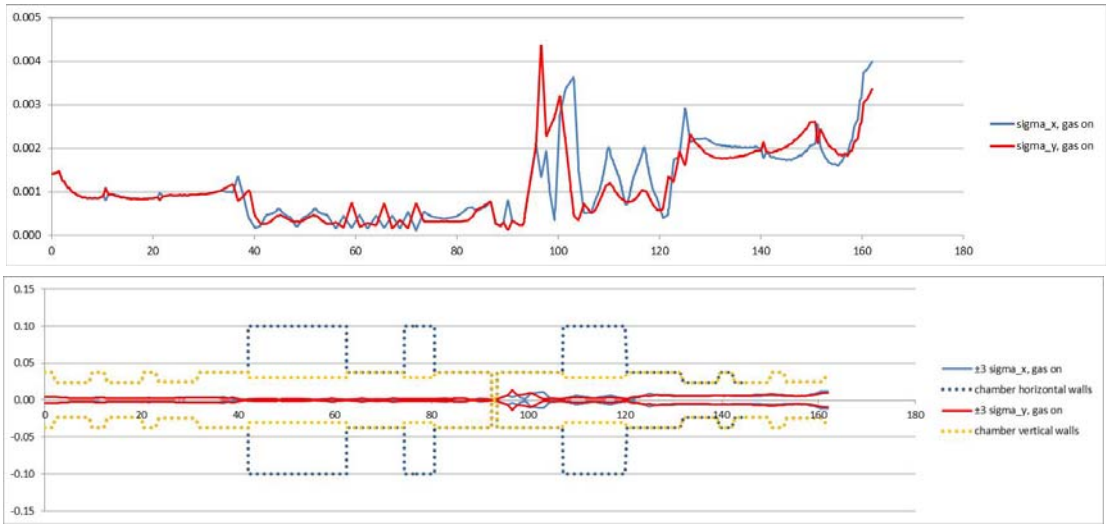

Figure 5. RMS beam envelopes for a thin target (top) and three times the RMS envelope compared to the beampipe aperture (bottom). All units are in meters.

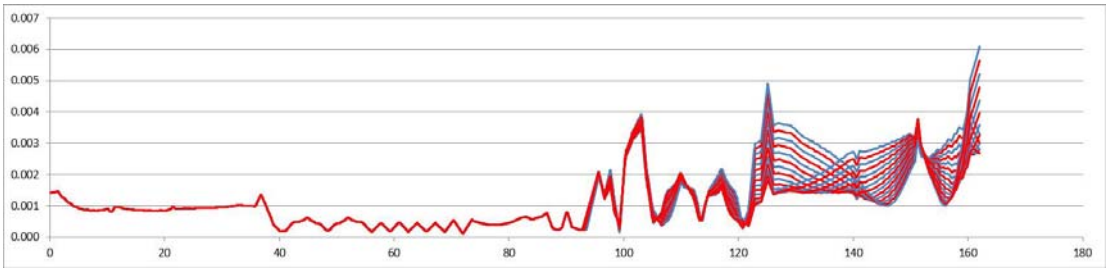

Figure 6. Beam envelopes for a thick target rematched to the dump. Compare to figure 5.

could be injected into the target while maintaining ion pumps at the end of the target region.

When we tried to put beam through the target however, we found two problems:

(i) The transverse field in the solenoid created an arcing trajectory through the target. It was possible to get the beam to go through the upstream and downstream sets of foils but the trajectory was not straight;

(ii) We found that one of the foils was mis-aligned by about 1 mm. This was enough to reduce the aperture to about 2 mm, which was too small for the electron beam to be transported cleanly through the target.

Though we could run pulsed beam with significant losses in the foils, we would not run CW beam.

6. Conclusions

The basic setup of an internal target was tested. It is a complicated experiment and requires significant commissioning time, which was not available. It is very important to test out the full beam transport at full current without foils or gas before target installation. This was not done. Once the beam transport is properly configured, the target can be installed and the beam

transported, first without gas and then with gas. Once clean transmission has been achieved, the current can be ramped up to its full value.

6.1. Acknowledgments
This material is based upon work supported by the U.S. Department of Energy, Office of Science, Office of Nuclear Physics under contract DE-AC05-06OR23177.

References

[1] D. Hasell et al. "The BLAST Experiment" 2009 Nucl. Instl and Meth. A603 247
https://doi.org/10.1016/j.nima.2009.01.131, and
R. J. Holt, "Nuclear Physics with internal targets in electron storage rings" AIP Conference Proceedings **161**, 138 (1987)
https://doi.org/10.1063/1.36883.
[2] P. Ilten et al., "Experiments and Facilities for Accelerator-Based Dark Sector Searches"
arXiv:2206.04220 [hep-ex] https://doi.org/10.48550/arXiv.2206.04220
[3] A. G. Ruggiero, "Intrabeam scattering in electron and proton storage rings (a review)", AIP Conference Proceedings **123**, 424 (1984)
https://doi.org/10.1063/1.34887.
[4] J. Balewski et al., "The DarkLight Experiment: A Precision Search for New Physics at Low Energies", arXiv:1412.4717 [physics.ins-det]
https://doi.org/10.48550/arXiv.1412.4717.
[5] S. Lee et al., "Design and operation of a windowless gas target internal to a solenoidal magnet for use with a megawatt electron beam", Nucl. Instr. and Meth. , **A 939** (2019) 46–54
https://doi.org/10.48550/arXiv.1903.02648
[6] C. Tennant "LERF – New Life for the Jefferson Laboratory FEL", Proceedings of ERL 2017, TUIACC001
http://jacow.org/erl2017/papers/tuiacc001.pdf
[7] D. Douglas "Beam Optics for Transverse Scattering Management In An ERL", JLAB-TN-12-046, 26 September 2012.
[8] C. Tschalaer, "Target Scattering Phase Space", Bates-internal report B/IR-16-01, 28 June 2016.
[9] D. Douglas, S. Benson, and C. Tennant, "A Simple (and Quite Possibly Incorrect) Description of Magnetized Beam Formation (That Gives the Right Answer Anyway. . .)" JLAB-TN-18-006,
D. Douglas, "Betatron Matching Magnetized Beams", JLAB-TN-15-026, and
D. Douglas, "Electron Optics for Cooling Insertions", JLAB-TN-16-046.
[10] D. Douglas "IR FEL Driver ERL Configuration for the DarkLight Aperture Test", JLAB-TN-13-009, 11 December 2012.
[11] R. Alarcon et al. "Transmission of Megawatt Relativistic Electron Beams Through Millimeter Apertures", Phys. Rev. Lett. 111 (2013) 164801
https://doi.org/10.48550/arXiv.1305.0199